RNA (1995), *1*:1009–1017. Cambridge University Press. Printed in the USA.

Determination of nucleotide distances in RNA by means of copper phenanthroline-generated hydroxyl radical cleavage pattern

THOMAS HERMANN and HERMANN HEUMANN
Max-Planck-Institut für Biochemie, D-82152 Martinsried, Germany

ABSTRACT

In contrast to the commonly used Fe(II)-EDTA, bis(orthophenanthroline)-copper(I) (OP-Cu) first generates hydroxyl radicals after binding to RNA. Due to diffusion, the hydroxyl radicals can cleave neighboring nucleotides in a distance *r* of up to 1.5 nm to the OP-Cu binding site. Using the known structure of $tRNA^{Phe}$ as a reference, we show that the hydroxyl radical cleavage pattern generated by a specifically bound OP-Cu shows a 1/*r* dependence on the distance of the cleaved nucleotide to the OP-Cu binding site. We propose that OP-Cu is a suitable probe for obtaining data on the distances between nucleotides in RNA, which can be used in modeling the structure of the examined RNA. However, this information is restricted to about three to four bases surrounding an OP-Cu binding site.

Keywords: chemical probing; molecular modeling; RNA structure; tRNA

INTRODUCTION

Interest in methods for RNA structure analysis has grown rapidly since the discovery of RNA molecules, such as ribozymes or guide-RNAs, that participate in catalytic processes. Chemical probing with modifying or nicking reagents is a valuable tool for structural analysis of RNA, as shown by numerous publications (reviewed in Krol & Carbon, 1989; Sigman & Chen, 1990; Westhof et al., 1990). In contrast to NMR and crystallography, which provide information about atomic distances and coordinates, respectively, the structural information resulting from chemical probing experiments is more complex, but also less complete. Depending on the type of probe, structural features, such as secondary structure elements, solvent accessibility, as well as neighborhood relationships between nucleotides, can be studied. However, there is no straightforward procedure to derive quantitative structural parameters from chemical probing data. Despite difficulties in quantification, chemical probing data have been proven valuable for developing working models, especially when used as a basis for molecular modeling (Westhof et al., 1990; Major et al., 1991; Malhotra et al., 1993). Although methods that permit a more quantitative interpretation of chemical probing data have been developed, such as symbolic programming (Malhotra et al., 1993), no satisfying procedure is available yet that yields direct structural information from such data. In this paper, we intend to show that 1,10-bis(orthophenanthroline)-copper(I) (OP-Cu) can be used as a probe for obtaining distance information of nucleotides within an RNA loop. In contrast to reagents, such as Fe(II)-EDTA, that do not bind to nucleic acid but act as a source of hydroxyl radicals generated in solution, OP-Cu starts its nicking activity after specific binding to the nucleic acid. Athough Fe(II)-EDTA gives information about the overall solvent accessibility of the residues within RNA (Latham & Cech, 1989), the OP-Cu cleavage pattern provides information about the local surrounding of the probe's binding site. The chemical mode of OP-Cu action by generating hydroxyl radicals after binding to nucleic acid is well established (Pope et al., 1982; Drew & Travers, 1984; Thederahn et al., 1989). This probe was extensively used to analyze double-stranded B-DNA (Drew, 1984; Pope & Sigman, 1984; Sigman & Chen, 1990) and single-stranded regions of RNA (Mazumder et al., 1992). Double-stranded RNA in A-form is not cleaved by OP-Cu (Murakawa et al., 1989). It was sug-

Reprint requests to: Hermann Heumann, Max-Planck-Institut für Biochemie, D-82152 Martinsried, Germany; e-mail: heumann@vms.biochem.mpg.de.

gested that the observed nicking specificity reflects differences in the binding capacity of nucleic acid to OP-Cu rather than differences in the accessibility of nucleotides (Sigman et al., 1985; Mazumder et al., 1992). However, there is no single binding mode that could account for the observed differences in OP-Cu cleavage. Two models were proposed for OP-Cu interaction with double-stranded B-form DNA. Both suggest that OP-Cu binds within the minor groove, one assuming intercalation (Stockert, 1989; Veal & Rill, 1989), the other one assuming nonintercalative binding (Thederahn et al., 1989). Both models are consistent with the observation that double-stranded A-form RNA is not cleaved due to the shallow minor groove that cannot accommodate the OP-Cu molecule. For single-stranded nucleic acid, no model for OP-Cu binding is available. There is evidence that well-organized structures are prerequisite for binding of OP-Cu, as pointed out by Sigman et al. (1985). However, details of these structures are unknown. It is a subject of this paper to analyze characteristics of RNA structure that permit specific OP-Cu binding. Using this information, we show that OP-Cu-generated hydroxyl radicals can provide information about internucleotide distances within RNA. Our method rests on the idea that the nicking intensity exhibited at a nucleotide is correlated with the distance of this nucleotide to the binding position of OP-Cu. This is consistent with the suggested mechanism of OP-Cu binding to nucleic acid, followed by diffusion of free radicals to nearby sugars (Drew, 1984). From theoretical considerations concerning the hydroxyl radical diffusion, we derived a linear inverse relation between distance and cutting efficiency.

For testing our theory, we chose $tRNA^{Phe}$ as a model system because its crystal structure is known. The observation of a characteristic hydroxyl radical cleavage pattern of nucleotides within the anticodon loop of this tRNA led us to propose a specific binding site for OP-Cu there. We calculated the spatial position of this site using experimental probing data, along with tRNA atomic coordinates from crystal structure analysis. Data obtained suggest a binding site compatible with partial intercalation of OP-Cu, which is termed "bookmarking" (Stockert, 1989; Veal & Rill, 1989). To test the feasibility of our theory for OP-Cu binding to RNA, we performed molecular mechanical and dynamical calculations on a complex of OP-Cu bound to a model RNA system representing the anticodon loop of $tRNA^{Phe}$. Generalizing the results from these calculations, we conclude that partial stacking of nucleotide side chains, as in the anticodon loop of $tRNA^{Phe}$, is a prerequisite for binding of OP-Cu to single-stranded RNA. Moreover, we propose a general method using band intensity data from probing experiments with OP-Cu for determining internucleotide distances around a discrete OP-Cu binding site. Referring to our model system $tRNA^{Phe}$, we derive criteria for identifying such binding sites in single-stranded RNA.

RESULTS

As a model system, $tRNA^{Phe}$ was treated with OP-Cu, as described in the Materials and methods. The resulting cleavage pattern was analyzed on a sequencing gel shown in Figure 1A (lane 5). The OP-Cu pattern shows enhanced cleavage in the regions around nt 18 and 35, in line with the view that OP-Cu-generated hydroxyl radicals cleave in single-stranded RNA (Murakawa & Nierlich, 1989; Mazumder et al., 1992). This is also confirmed by previous experiments of Murakawa et al. (1989), where OP-Cu has been used to probe $tRNA^{Phe}$. The OP-Cu concentration used in our experiment is a factor of 10 lower than that used previously by these authors. Therefore, we achieved an increased contrast between few specific binding sites for OP-Cu and background cutting: the resulting pattern depicts essentially only the most prominent cleavage spots, namely around nt 18 and 35. In order to ensure that the pattern is obtained from a homogeneous population of $tRNA^{Phe}$

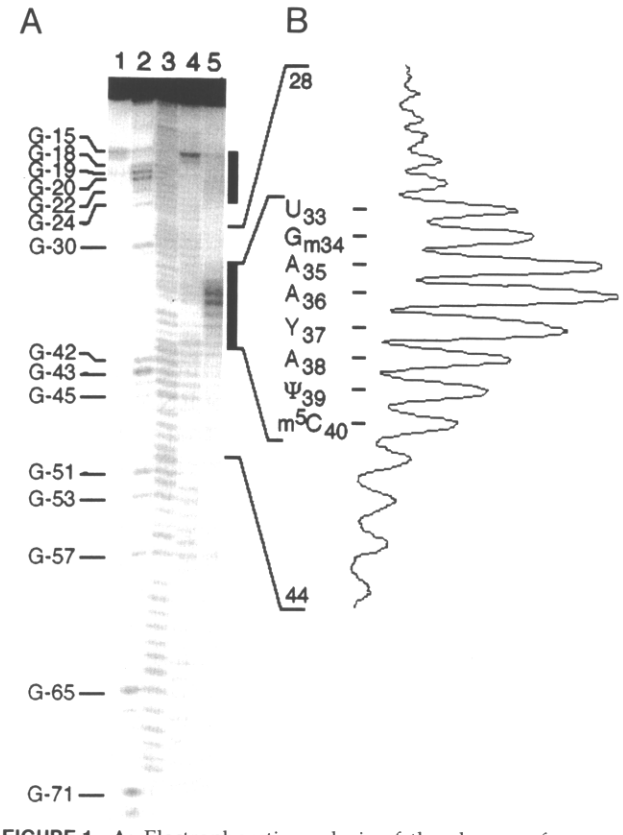

FIGURE 1. A: Electrophoretic analysis of the cleavage fragments from treatment of $tRNA^{Phe}$ with OP-Cu (lane 5) shows two reactive regions, namely around nucleotide positions 18 and 35, marked on the right side. Lane 1, controls with untreated $tRNA^{Phe}$; lane 2, $tRNA^{Phe}$ treated with G-specific T1-nuclease; lane 3, partial alkaline hydrolysis conditions; lane 4, Fe(II)-EDTA-generated hydroxyl radicals. At G_{15}, enhanced cleavage, probably due to pH-dependent hydrolysis, is observed in the Fe(II)-ETDA reaction and also, yet to a lesser extent, in the control lane with untreated RNA. **B:** Densitometric scan of the OP-Cu cleavage reaction (A, lane 5) is shown with background subtracted in the region of nt C_{28}–A_{44}. The pattern of enhanced cleavage around nt A_{35} and A_{36} was used for calculation of the cleavage intensities by integration of peak areas.

molecules, the untreated tRNA is shown as a reference as well as the RNase T1 pattern (Fig. 1A, lanes 1, 2). For further analysis, we have chosen the OP-Cu pattern of the anticodon loop around nt 35, because these bands are well-resolved, as indicated by the densitometric scan of this region ranging from nt U_{33} to m^5C_{40} (Fig. 1B). Two intense bands, representing nt 35 and 36, are flanked by a series of bands of decreasing intensity. There are two possible binding modes of OP-Cu that could explain the observed pattern. One possibility is that Op-Cu molecules can bind to several positions in the anticodon loop. The differences in the band intensities would then reflect different affinities of OP-Cu to the binding sites in the anticodon loop. Another possibility is that Op-Cu is bound at one position in the anticodon loop close to nt 35 and 36. The intensity of the bands would then reflect the distance between the hydroxyl radical-generating OP-Cu molecule and the cleaved nucleotide. The idea that a probe that is specifically bound to RNA preferentially cleaves the nucleotides in proximity to the probe's binding site is not new, as pointed out by Chu and Orgel (1985) and also by Wang and Cech (1992). These authors also suggested that the pattern obtained by site specifically bound Fe(II)-EDTA, attached either to guanosine triphosphate (Wang & Cech, 1992) or to short oligodeoxynucleotides (Chu & Orgel, 1985), can be explained by distance-dependent cleavage of diffusible hydroxyl radicals. We follow their view and assume that the varying intensity of the bands in the $tRNA^{Phe}$ anticodon loop is due to the cleavage activity of diffusible hydroxyl radicals generated by an OP-Cu specifically bound between nt 35 and 36. The variation of the cleavage intensity should then reflect the concentration of hydroxyl radicals, which decreases with increasing distance from the putative OP-Cu binding site.

We suggest that the mechanism accounting for the observed high specificity of OP-Cu within the $tRNA^{Phe}$ anticodon loop is partial intercalation, or bookmarking. This type of interaction avoids sterical repulsion, because the base side chains project into the solvent, thus forming a hydrophobic surface region on $tRNA^{Phe}$ suitable for binding of OP-Cu. We tested our hypothesis of distance-dependent cleavage by OP-Cu-generated hydroxyl radicals in two steps. First, a quantitative expression for the concentration of hydroxyl radicals $[R^*]$ depending on the distance r to the source, namely the OP-Cu molecule, was evaluated. Second, the derived expression for $[R^*](r)$ was applied to the cleavage pattern in the $tRNA^{Phe}$ anticodon loop to test whether the observed intensities were compatible with our model.

Determination of relative distances of the cleaved nucleotides to the putative OP-Cu binding site

The function $[R^*](r)$ was derived by using Fick's first law (Equation 1), which assumes that diffusion is driven by a concentration gradient of the diffusing species:

$$d[R^*] = \frac{-J}{4\pi D_B N_A} \cdot \frac{dr}{r^2}, \quad (1)$$

(where J is the flux, D_B is the diffusion constant, and N_A is Avogadro's number).

We can apply this law, although each OP-Cu molecule generates only one hydroxyl radical per binding event rather than a steady flux. Our system, consisting of an ensemble of OP-Cu/RNA complexes, can be equivalently described by a point source producing a constant flux of radicals. The assumption of a constant radical flux is justified because, under the experimental conditions, the probing reagent OP-Cu acts as a redox catalyst that is continuously restored due to the influence of reducing agents.

Considering that for $r \to \infty$, the concentration of particles reaches zero, integration of Equation 1 results in an inverse proportionality between the hydroxyl radical concentration $[R^*]$ and the distance r to the source:

$$[R^*]_r = \frac{-J}{4\pi D_B N_A} \cdot r^{-1}. \quad (2)$$

It is plausible to assume that the cleavage probability, P_c, is proportional to the concentration of hydroxyl radicals. Accordingly, Equation 2 reads:

$$P_c = q \cdot r^{-1}, \quad (3)$$

where q is a proportionality factor.

The cleavage probabilities, P_c, depicted in Table 1 were determined as the integrated band intensities, A_i, of Figure 1A (lane 5). The distances, r_i, of the corresponding nucleotides in the anticodon loop were calculated by using the atomic coordinates from the available X-ray structure of $tRNA^{Phe}$. The proportionality factor, q, was obtained from band intensities and distances, as described in the Materials and methods. The position is located between the base side chains of A_{35} and A_{36}, in line with our assumption that the radical-generating OP-Cu is bound between A_{35} and A_{36}. The average value of q obtained from the fitting procedure was determined as $q = 4.53 \pm 0.45$.

The observed linear relationship of the distances derived from the crystal structure and the cleavage prob-

TABLE 1. Cleavage probabilities for nt U_{33}–Ψ_{39}.

Nucleotide	Cleavage probability $P_c = A_i$	Distance $C_{1'} \to Cu$ r_i (Å)	Proportionality factor q
U_{33}	0.46	9.4	4.36
G_{34}	0.48	10.6	5.09
A_{35}	0.80	6.6	5.29
A_{36}	1.00	4.3	4.30
Y_{37}	0.72	6.5	4.70
A_{38}	0.38	11.2	4.21
Ψ_{39}	0.28	14.9	4.14
m^5C_{40}	0.22	18.9	4.16

abilities indicates that the RNA structure around the reagent's binding site does not change essentially upon OP-Cu binding. In the following section, we addressed this topic from a theoretical point of view.

Analysis of a possible conformational change of the anticodon loop due to OP-Cu binding

The approach described above for the determination of the OP-Cu binding site rests on the assumption that the structure of the anticodon loop is not essentially disturbed upon binding of OP-Cu. In order to verify this assumption, Op-Cu was docked to $tRNA^{Phe}$ between base position 35 and 36 using molecular modeling techniques and molecular dynamics (MD) calculations. The deviation of the calculated structure, containing OP-Cu, from the original X-ray structure, was determined.

For positioning OP-Cu, a least-squares plane equidistant to the planes through the base side chains of A_{35} and A_{36} was calculated. For a starting position, OP-Cu was placed in a way that one of the phenanthroline ligands coincided with the least-squares plane. Subsequently, we minimized the system in vacuo to an RMS gradient below 1.0 kcal/molÅ employing 25 steps of SIMPLEX algorithm to remove high strain, followed by the usual conjugate gradient procedure. The nt G_{24}–G_{30} and m^5C_{40}–G_{42} within the stem were kept rigid during this minimization procedure, whereas the loop nt A_{31}–Ψ_{39} and intercalated OP-Cu were allowed to relax freely. Using this approach, two main conformations of the OP-Cu bound between the base side chains of A_{35} and A_{36} were found, which we termed "facial complex" and "angular complex" (Fig. 2A). We chose the angular complex for the following dynamics calculations because this complex yielded a lower energy in minimization calculations due to less sterical hindrance. Inspection of the angular complex reveals that OP-Cu is bound from the minor groove side of the bases, in line with previously published models for the binding of OP-Cu to DNA (Stockert, 1989; Thederahn et al., 1989; Veal & Rill, 1989). The shallow minor groove of the A-form anticodon stem continuously merges into the exposed base stack of the single-stranded loop region, where the binding of OP-Cu via an intercalative mode is possible.

Comparison of the resulting structure of the tRNA with that obtained from the X-ray data indicates only a minimal change in the overall geometry of the anticodon loop upon intercalation of OP-Cu (Fig. 2B). In particular, the spatial position of the backbone sugars is affected minimally only.

MD simulation of OP-Cu bound to the anticodon loop of $tRNA^{Phe}$

Using MD simulations, we addressed the question whether partial intercalation of OP-Cu between A_{35} and A_{36} is a reasonable binding mode. For that purpose, the angular OP-Cu/RNA complex described above was simulated in a solvent environment. For compensation of the negative charges on the phosphate backbone, 17 Na^+ counterions were added. All but one of the sodium ions were positioned bisecting the charged oxygens of the respective phosphate group at a distance of 4 Å to phosphorous. Due to sterical reasons, the counterion of G_{m34} was placed differently. The electrostatic potential around the respective phosphate group was calculated and the sodium counterion was positioned outside the loop at the point of lowest potential. In addition, the complex contained a single magnesium ion, accounting for two negative charges. This magnesium ion, resolved in the crystal

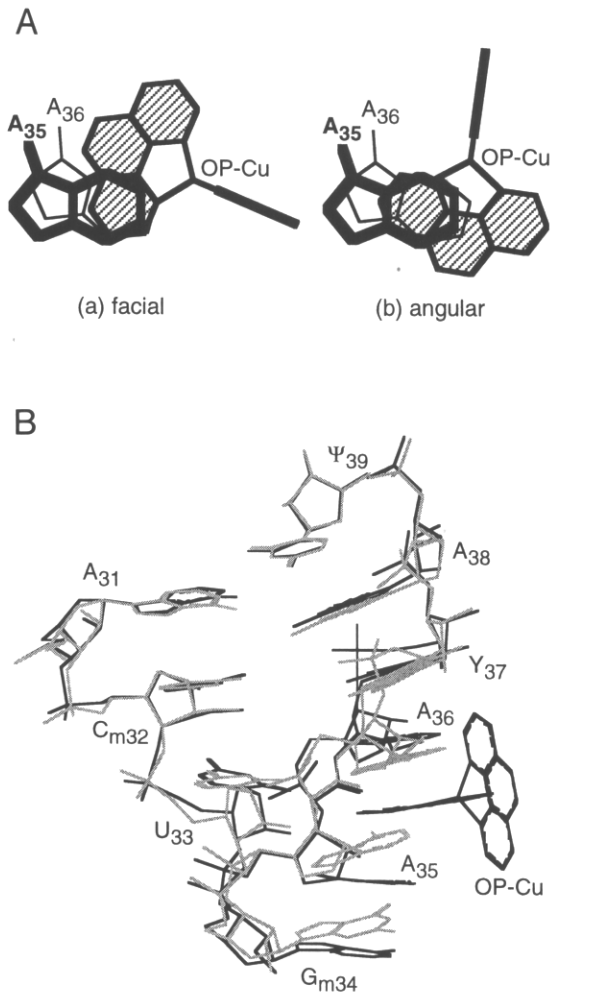

FIGURE 2. **A:** Docking of OP-Cu between the base side chains of A_{35} and A_{36} results in two different conformations: (a) the facial complex, and (b) the angular complex. The angular complex was chosen for all further simulations, because it resulted in less sterical hindrance between RNA and the OP-Cu molecule. **B:** Refined angular complex of OP-Cu and RNA displays only a minimal change in the RNA backbone geometry when compared to the crystal structure of the $tRNA^{Phe}$ that was used as a starting point for docking of OP-Cu. The complex is shown in black, the unperturbed tRNA in grey. Only nt A_{31}–Ψ_{39} are depicted.

structure, is located within the anticodon loop. Solvation of the complex was accomplished by immersing it in a periodic box of TIP3P water. Energy refinement of solvent and solvate gave the starting system for the following MD calculation.

As a measure for the quality of the dynamics simulation, the integrity of the OP-Cu/RNA complex was checked. Therefore, different parameters, describing both the geometry of the anticodon loop RNA as well as the binding of OP-Cu, were monitored continuously, namely the groove width of the RNA, its radius of gyration, and the distance of the OP-Cu molecule to neighboring nucleotides. As one would expect, the initial radius of gyration of the RNA (14 Å) increased while the system was heated in the beginning of the calculation. Later, the radius of gyration stabilized and oscillated around 15 Å. From the plot of groove widths (Fig. 3A), it follows that the anticodon loop remained stable during dynamics calculation. This finding is confirmed in detail by the stable behavior of the conformational angles, the ribose δ torsions, and the base χ torsions. Similar results were obtained when the MD calculation was performed on the pure RNA system without intercalated OP-Cu (data not shown). However, when simulations were done without explicit treatment of the hydrated magnesium ion, collapse of the loop structure was observed frequently. These instabilities of the counterion-free loop occurred with, as well as without, OP-Cu intercalated. Alternative treatment of the magnesium ion by a hydrated counterion with artificially enlarged radius, as described for hydrated sodium ions by Singh et al. (1985), was not successful, because the large ion tended to expand the loop structure. Thus, explicit treatment of the water molecules coordinated to the magnesium was necessary. It is interesting to note that, during the dynamics calculation, exchange of water from the hydrate shell with water from the bulk solvent was observed (Fig. 3B). The magnesium ion itself remained close to the phosphate, where it is found in the X-ray structure.

In order to monitor the binding of OP-Cu to the RNA, the distance from the central Cu to the $C_{1'}$ atoms of the flanking nucleotides forming the intercalation site was recorded (Fig. 3C). Over the simulation period, the OP-Cu stays permanently between the base side chains of the intercalation site, indicating that partial intercalation could stabilize an OP-Cu molecule on RNA. This was also confirmed by the van der Waals interaction between the RNA and OP-Cu, which oscillated steadily around 30 kcal/mol during the entire simulation.

In order to support our view that the binding site between the nucleotides at positions 35 and 36 is the strongest one for OP-Cu, the neighboring nucleotides forming the base stack in the anticodon loop were inspected. The stacked nt G_{m34}/A_{35} and A_{36}/Y_{37} could, in principle, provide sites for intercalative binding of OP-Cu. However, binding between A_{36} and Y_{37} is less

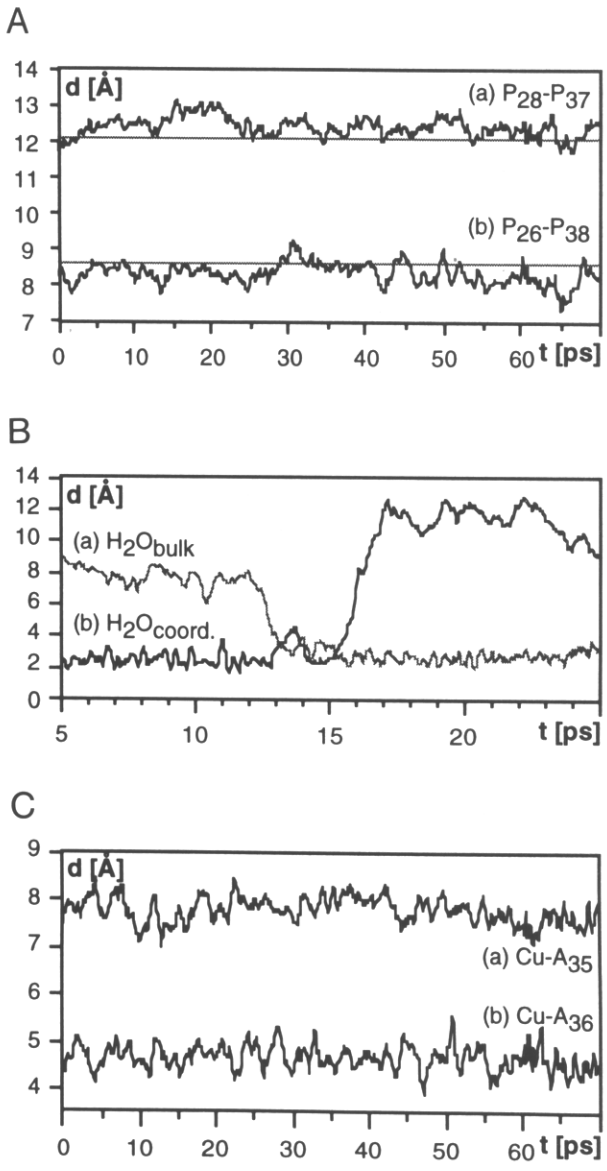

FIGURE 3. **A:** RNA groove widths during the 70-ps MD simulation at 300 K were monitored as the distances between facing phosphates of nt C_{28} and Y_{37} (a, P_{28}–P_{37}), and G_{26} and A_{38} (b, P_{26}–P_{38}), respectively. The respective distances in the crystal structure of $tRNA^{Phe}$ are marked in grey. The plot shows that the model RNA loop remained stable during dynamics simulation. **B:** Exchange of water coordinated to the magnesium ion within the model RNA loop was observed during the MD simulation. Oxygen–metal distances were recorded for a water molecule from the coordination sphere of magnesium (b, $H_2O_{coord.}$) that is replaced by a water molecule from the bulk solvent (a, H_2O_{bulk}). **C:** Distances between Cu of OP-Cu and the $C_{1'}$ atoms of A_{35} (a, Cu-A_{35}) and A_{36} (b, Cu-A_{36}) forming the OP-Cu bookmarking site as monitored during the MD simulation. The plot shows that the OP-Cu molecule stays permanently between the base side chains of the binding site.

favorable due to the bulkiness of the side chain of the modified base Y_{37}. Moreover, the site between positions 34 and 35 was ruled out as a binding location for OP-Cu because the side chain of G_{m34} at the tip of the anticodon loop displayed a high flexibility in dynamics calculations. From position 38 to farther up the anti-

codon loop, the stacking bases are increasingly shielded inside the groove of the A-form RNA helix forming there, and intercalation of OP-Cu is not possible. As pointed out previously, the shallowness of the minor groove prevents OP-Cu from binding to double-stranded A-form RNA.

In summary, we have shown that a binding site for OP-Cu found on $tRNA^{Phe}$ by quantification of probing data is compatible with a partial intercalative mode of binding (bookmarking). Using molecular modeling techniques, OP-Cu was successfully docked to the experimentally determined binding site in the anticodon loop of $tRNA^{Phe}$ between A_{35} and A_{36}. As we demonstrated for partial intercalation of OP-Cu, no drastic change of the anticodon loop geometry is necessary. Results of MD calculations further indicated that bookmarking could provide a stable mode of binding for OP-Cu between A_{35} and A_{36}.

DISCUSSION

Using $tRNA^{Phe}$ as a model system, we show that the chemical probe OP-Cu can be used to obtain information about internucleotide distances in RNA. OP-Cu acts through generation of hydroxyl radicals that cleave RNA at the sugar moieties. Prerequisite for the probing activity of OP-Cu is binding of the reagent to the RNA. In agreement with previous statements in the literature (Drew, 1984; Wang & Cech, 1992), we propose that hydroxyl radicals produced by bound OP-Cu cleave RNA in a distance-dependent manner. The results we obtained by quantitation of the OP-Cu generated cleavage pattern in the anticodon loop of $tRNA^{Phe}$ are in line with this view. The region of enhanced cleavage comprises eight nucleotides, from position 33 to 40, with most intense cutting at positions 35 and 36. We interpret this pattern by assuming: (1) that an OP-Cu binding site is located between the most efficiently cleaved nt 35 and 36; and (2) that decaying nicking intensity at nucleotides flanking the radical source is due to diffusion of hydroxyl radicals. The radical concentration decreases proportional to the distance from the source according to Fick's law and, therefore, cleavage efficiency at a nucleotide is inversely proportional to the distance between the cleaved nucleotide and the location of the radical source, as outlined in the Results. The distances of nt 33–40 to the bound OP-Cu between position 35 and 36 calculated from the experimentally determined cleavage pattern are compatible with the respective distances derived from the crystal structure of this tRNA, indicating that the assumptions made above are justified.

It was our aim to show that it is possible to use the OP-Cu cleavage pattern to obtain distance information within an RNA molecule with unknown three-dimensional structure. In order to demonstrate the usefulness of our approach, we analyzed the OP-Cu-derived pattern of $tRNA^{Phe}$ in Figure 1A (lane 5) without taking advantage of the known atom coordinates of $tRNA^{Phe}$. The following conditions must be fulfilled before the evaluation of an OP-Cu-dependent pattern by our method can provide reliable results. (1) The RNA used for the probing experiment must be a homogeneous intact species with a purity of better than 98%. This was checked by electrophoretic analysis of untreated RNA (Fig. 1A, lane 1) and of T1-nuclease-digested RNA (Fig. 1A, lane 2). The latter shows clear single bands at G-positions. (2) The concentration of OP-Cu has to be low enough to ensure single hit conditions. (3) The analyzed cleavage pattern must be generated by hydroxyl radicals diffusing from OP-Cu bound at one single position. Therefore, the reagent concentration has to be sufficiently low to avoid contribution of unspecifically bound OP-Cu. Enhancement of the pattern in the anticodon loop $tRNA^{Phe}$ was achieved by using an OP-Cu concentration 10-fold less than that reported previously by Murakawa et al. (1989). (4) Superposition of patterns due to neighboring OP-Cu molecules bound on RNA at a distance of less than 5 nt should be avoided because interpretation is more complicated then. We have, therefore, chosen the cleavage pattern of the anticodon loop in our analysis of $tRNA^{Phe}$. This pattern is the most distinctive, being clearly separated from the other patterns, and having a well-defined intensity maximum around nt 35 and 36, which are flanked by nucleotides cleaved with smoothly decreasing efficiency. For the quantification of the cleavage efficiency, it is important to correct the pattern for background effects, as described in the Materials and methods.

When analyzing the cleavage pattern of an RNA of unknown structure, there is no direct way to determine the exact binding position of OP-Cu. However, as a starting point, it can be assumed that the OP-Cu molecule intercalates like a bookmark between the two most strongly cleaved nucleotides. The validity of this assumption was verified in the case of $tRNA^{Phe}$ by energy minimization and MD calculations, which show that OP-Cu is likely to interact with RNA in an intercalative mode between position 35 and 36.

Our suggestion that a transition from the single-stranded region of an RNA loop to a helical region is a preferential binding site for OP-Cu via intercalative binding between stacked bases might also explain probing data of other authors. RNAs that show enhanced OP-Cu cleavage at such stem/loop sites were the TAR region of HIV (Mazumder et al., 1992) and the 5′ untranslated regulatory region of ferritin mRNA (Wang et al., 1990).

Provided that the two most strongly cleaved nucleotides were identified, interactively placing OP-Cu between them fixes the distance of OP-Cu to the neighboring nucleotides and thus determines the proportionality factor q. Using q allows the calculation of distances r_i from the band intensity according to Equation 3,

where cleavage probabilities P_c were substituted by band intensities A_i. The values obtained represent the distances between the center of the OP-Cu bookmarking site and the cleaved nucleotides' $C_{1'}$ atoms, the preferred cleavage site of hydroxyl radicals (Sigman & Chen, 1990).

The statistical accuracy of the distance values depends on the accuracy of the intensity determination of the bands as a measure of the cleavage efficiency. It is, in our case, around 5%. In addition, an unknown systematic error is introduced by positioning of the OP-Cu molecule between the base side chains of two nucleotides. An upper limit of the margin of this systematic error is the size of the OP-Cu binding site, which is around half the distance between stacking base side chains of neighboring nucleotides.

The obvious conclusion that can be drawn from the distance values is indicated in Figure 4, namely, whether the probed RNA region deviates from a straight stretch. However, the main advantage of the obtained distances is their use for confining the conformational space of the probed RNA region in modeling of RNA from additional solution-probing data. We are aware of the fact that the few obtained distances are not sufficient to fully determine the structure of the probed RNA region. They rather limit the number of possible conformations.

There are many examples that show that chemical probing data are helpful in computer-aided molecular modeling studies on RNA (e.g., Westhof et al., 1990; Felden et al., 1994; Tanner et al., 1994). Treatment of OP-Cu cleavage patterns introduced here can provide very specific information about the relative distances between nucleotides in an RNA structure, and should therefore prove to be a particularly powerful accessory technique for RNA structure modeling.

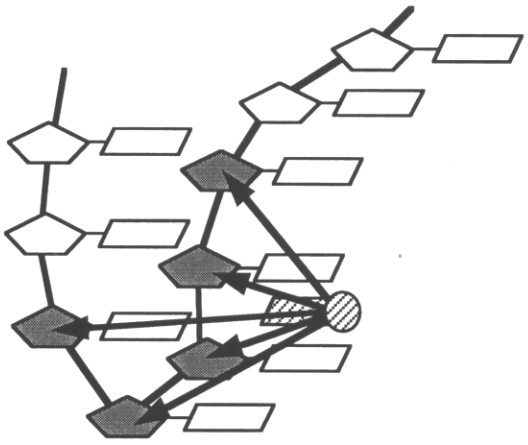

FIGURE 4. Chemical probe OP-Cu (hatched circle) produces diffusible hydroxyl radicals after binding to RNA resulting in distance-dependent cleavage around the reagent's binding site. Nucleotides situated close to the reagent due to curvature or looping of the single-stranded RNA are more intensely cleaved (grey) than they would be when located in straight RNA.

MATERIALS AND METHODS

Preparation of RNA

Yeast $tRNA^{Phe}$ (Boehringer Mannheim) was 3'-end-labeled with [^{32}P]pCp (Amersham) using T4 RNA-ligase (Boehringer Mannheim) as described (England et al., 1980). Both labeled and unlabeled RNA were purified by electrophoresis on 5% acrylamide gels containing 8% urea, where UV-shadowing was employed for band identification when working with unlabeled RNA. Bands containing correct-sized RNA were cut from the gels and the product was recovered in 500 mM ammonium acetate/0.1% SDS buffer.

Probing experiments

Probing experiments were performed as described in the literature (Murakawa et al., 1989; Wang et al., 1990; Mazumder et al., 1992). A concise review of practical aspects of the use of OP-Cu in chemical probing is given by Papavassiliou (1994).

In our experiments, 100 ng of unlabeled tRNA were mixed with 50.000 cpm of labeled RNA in 20 μL of 50 mM Tris/HCl buffer, pH 7.9, containing 10 mM $MgCl_2$ and 50 mM NaCl.

OP-Cu reagent was formed from 40 μM phenanthroline, 20 μM copper(II)sulfate, and 5 mM mercaptopropionic acid, along with 7 mM of hydrogen peroxide. After reaction at 37 °C for 5 min, a quenching solution containing an excess of 2.9-dimethyl-ortho-phenanthroline was added, followed by ethanol precipitation of RNA. Analysis of RNA fragments was done on 12% polyacrylamide gels.

Determination of the OP-Cu binding position

X-ray films of the electrophoresis gels with the probing pattern were scanned on a Hirschmann photodensitometer. Band intensities A_i were calculated as Gaussian peak areas from the densitometer scans after subtracting background intensity.

The position of OP-Cu $P(x_P\, y_P\, z_P)$ was calculated assuming an inverse proportionality of the distance r_i from the reagents binding site to the $C_{1'}$ atom of the ith nucleotide $P(x_i\, y_i\, z_i)$ and the respective cutting efficiency determined from the band intensity A_i, as noted in the Results. The band intensities of the nt U_{33}–m^5C_{40} in the anticodon loop of $tRNA^{Phe}$, showing enhanced cleaving, were used to determine the proportionality factor q, converting A_i to r_i according to $r_i = qA_i$, with $r_i = \sqrt{(x_P - x_i)^2 + (y_P - y_i)^2 + (z_P - z_i)^2}$. The atomic coordinates used for these calculations were taken from the $tRNA^{Phe}$ PDB-file 4TRA from the Brookhaven Protein Data Bank (Sussman et al., 1978; Westhof et al., 1988).

Modeling studies

Molecular mechanics and dynamics calculations were performed using the SYBYL molecular modeling environment (Tripos Assoc., St. Louis, Missouri). Semiempirical quantum mechanical calculations were done with MOPAC (6.0, Quantum Chemistry Program Exchange Program #455). For all pro-

cedures based on molecular mechanics, the AMBER force field supplied with SYBYL software was applied throughout (Weiner et al., 1984).

Parametrization of OP-Cu

For all atoms of the complex, we introduced new AMBER atom types. The force field parameters were chosen in accordance with already existing parameters from the literature (Lybrand et al., 1986; Weiner et al., 1986; Abraham et al., 1988). Parameters for Cu were $r_{\text{van der Waals}} = 0.96$ Å, $\epsilon_{well} = 0.01$ kcal/mol.

The partial atomic charges for OP-Cu were derived by fitting to the electrostatic potential calculated from the semiempirical PM3 wave function (Singh & Kollman, 1984). To account for both the distribution of the positive charge of Cu on the ligands and the poor representation of a heavy element such as Cu in quantum mechanical calculations, we employed a modified method of Haworth et al. (1991). Thus, we used electrostatic potentials obtained from the respective PM3 wave functions of phenanthroline (Ph) itself and an *N,N'*-diprotonated (H_2Ph) phenanthroline ion: the excess charges on the single atoms of H_2Ph were obtained by subtracting the charges of Ph. They were scaled by 0.5 to account for the fact that Cu is singly charged. The resulting scaled excess charges were added to the charges on Ph. From this artificial singly charged system, we calculated how much of the charge is transferred from additional protons to phenanthroline ligands. Half of this total transferred charge would be located on each of the two ligands in the copper complex. Thus, we obtained the final partial atomic charges for one phenanthroline ligand by summing 50% of the charges from phenanthroline and 50% of scaled H_2Ph atomic charges for each atom.

Modeling of RNA

In order to model the anticodon loop of $tRNA^{Phe}$, we started from atomic coordinates of the crystal structure (Sussman et al., 1978; Westhof et al., 1988). All modified nucleotides, along with the water plus four Mg^{++} ions, were retained from the X-ray structure. AMBER atom types and force field parameters for the modified nucleotides were assigned following data for similar cases from the literature (detailed data can be obtained on request from the authors) (Weiner et al., 1986; Allen et al., 1987). Atomic partial charges for the modified nucleotides' sugar moieties were taken from the standard nucleotides. Charges for the base side chains of nonstandard nucleotides were calculated according to the Pullman method implemented in the SYBYL package.

Water was represented with TIP3P model water (Jorgensen et al., 1983). The parameters for the Mg^{++} ions were $r_{\text{van der Waals}} = 1.17$ Å, $\epsilon_{well} = 0.1$ kcal/mol (Aqvist, 1990). We added hydrogens to the RNA, employing a built-in algorithm of SYBYL and subsequently energy-refined the hydrogens, whereas all heavy atoms were fixed as an aggregate. We chose a distance-independent dielectric constant of $\epsilon = 1$ and a 10-Å cutoff for nonbonded interactions. Refinement was done until the RMS gradient dropped below 0.1 kcal/molÅ. From the refined structure, we removed all the water molecules and nt G_1–A_{23} and G_{43}–A_{76}. The structure from G_{24} to G_{42} plus one magnesium ion, situated in the anticodon loop, along with five molecules of water coordinated to this ion, were retained. The two ends of the model anticodon loop (5′-G_{24} and 3′-G_{42}) were capped with hydroxyl groups.

The resulting structure was used for all further steps of calculation.

Docking of OP-Cu to the RNA

Docking of OP-Cu to the RNA was performed manually employing the "Docking" environment implemented in SYBYL. The reagent was moved until the continually monitored energy of interaction between RNA and OP-Cu was optimal, i.e., until the energy of repulsion was lowest and the energy of attraction was highest.

Preparation of the solvated system

Na^+ counterions ($r_{\text{van der Waals}} = 1.87$ Å, $\epsilon_{well} = 0.0028$ kcal/mol) (Aqvist, 1990) were used to compensate for the charges on the RNA backbone.

The system was solvated by immersing it in a cubic box of TIP3P water molecules obtained by a Monte Carlo simulation of liquid water (Jorgensen et al., 1983). Such solvent molecules were removed where the oxygen was within the van der Waals radius of any non-hydrogen of the solvate. The final box size was 45.1 Å after adjusting to an overall density of 1.0 g/cm^3. The box contained 2,600 solvent molecules. In order to remove bad contacts between solvent molecules at the box interfaces due to the applied periodic boundary conditions, we energy-refined the whole system to an RMS gradient of 0.1 kcal/molÅ.

MD calculations of the solvated OP-Cu/RNA complex

During MD calculations, the stem RNA, consisting of nt G_{24}–G_{30} and m^5C_{40}–G_{42}, was constrained to the X-ray structure, whereas no constraints were put on the loop RNA (nt A_{31}–Ψ_{39}) nor on OP-Cu. A time step of 1 fs was used throughout. The solvated OP-Cu/RNA system was heated to the final simulation temperature of 300 K in steps of 50 K during 30 ps by coupling to an external bath every 200 fs (Berendsen et al., 1984). Random values were assigned as starting velocities following a Maxwellian distribution at 10 K. Following the heating procedure, we performed a 70-ps MD calculation at constant temperature of 300 K, where coupling to the external bath was done every 300 fs. Data were collected every 150 fs.

ACKNOWLEDGMENTS

We thank Matthias Götte for providing tRNA probing data and Dr. Andrew Wedel for valuable discussion during preparation of the manuscript. T.H. thanks the Studienstiftung des deutschen Volkes for support. This work was supported by the Deutsche Forschungsgemeinschaft.

Received October 5, 1995; returned for revision October 13, 1995; revised manuscript received November 3, 1995

REFERENCES

Abraham ZHL, Agbandje M, Neidle S, Acheson RM. 1988. Experimental DNA-binding and computer modelling studies on an analogue of the anti-tumour drug amsacrine. *J Biomol Struct Dynam 6*:471–488.

Allen FH, Kennard O, Watson DG, Brammer L, Orpen AG, Taylor R. 1987. Tables of bond lengths determined by X-ray and neutron diffraction. *J Chem Soc Perkin Trans II*:S1–S19.

Aqvist J. 1990. Ion–water interaction potentials derived from free energy perturbation simulations. *J Phys Chem 94*:8021–8024.

Berendsen HJC, Postma JPM, van Gunsteren WF, DiNola A, Haak JR. 1984. Molecular dynamics with coupling to an external bath. *J Chem Phys 81*:3684–3690.

Chu BCF, Orgel LE. 1985. Nonenzymatic sequence-specific cleavage of single-stranded DNA. *Proc Natl Acad Sci USA 82*:963–967.

Drew HR. 1984. Structural specificities of five commonly used DNA nucleases. *J Mol Biol 176*:535–557.

Drew HR, Travers AA. 1984. DNA structural variations in the *E. coli tyrT* promoter. *Cell 37*:491–502.

England TE, Bruce AG, Uhlenbeck OC. 1980. Specific labeling of 3′ termini of RNA with T4 RNA ligase. *Methods Enzymol 65*:65–85.

Felden B, Florentz C, Giege R, Westhof E. 1994. Solution structure of the 3′-end of Brome mosaic virus genomic RNAs. *J Mol Biol 235*:508–531.

Haworth IS, Elcock AH, Freeman J, Rodger A, Richards WG. 1991. Sequence selective binding to the DNA major groove: Tris(1,10-phenanthroline) metal complexes binding to poly(dG-dC) and poly(dA-dT). *J Biomol Struct Dynam 9*:23–44.

Jorgensen WL, Chandrasekhar J, Madura JD, Impey RW, Klein ML. 1983. Comparison of simple potential functions for simulating liquid water. *J Chem Phys 79*:926–935.

Krol A, Carbon P. 1989. A guide for probing native small nuclear RNA and ribonucleoprotein structures. *Methods Enzymol 180*:212–227.

Latham JA, Cech TR. 1989. Defining the inside and outside of a catalytic RNA molecule. *Science 245*:276–282.

Lybrand TP, Brown SC, Creighton S, Shafer RH, Kollman PA. 1986. Computer modeling of actinomycin D interactions with double-helical DNA. *J Mol Biol 191*:495–507.

Major F, Turcotte M, Gautheret D, Lapalme G, Fillion E, Cedergren R. 1991. The combination of symbolic and numerical computation for three-dimensional modeling of RNA. *Science 253*:1255–1260.

Malhotra A, Gabb HA, Harvey SC. 1993. Modeling large nucleic acids. *Curr Opin Struct Biol 3*:241–246.

Mazumder A, Chen CB, Gaynor R, Sigman DS. 1992. 1,10-Phenanthroline-copper, a footprinting reagent for single-stranded regions of RNA. *Biochem Biophys Res Commun 187*:1503–1509.

Murakawa GJ, Chen CB, Kuwabara MD, Nierlich DP, Sigman DS. 1989. Scission of RNA by the chemical nuclease of 1,10-phenanthroline-copper ion: Preference for single-stranded loops. *Nucleic Acids Res 17*:5361–5375.

Murakawa GJ, Nierlich DP. 1989. Mapping the *lacZ* ribosome binding site by RNA footprinting. *Biochemistry 28*:8067–8072.

Papavassiliou AG. 1994. 1,10-Phenanthroline–copper ion nuclease footprinting of DNA–protein complexes in situ following mobility-shift electrophoresis assays. In: Kneale GG, ed. *Methods in molecular biology 30*. Totowa, New Jersey: Humana Press. pp 43–78.

Pope LE, Sigman DS. 1984. Secondary structure specificity of the nuclease activity of the 1,10-phenanthroline–copper complex. *Proc Natl Acad Sci USA 81*:3–7.

Pope LM, Reich KA, Graham DR, Sigman DS. 1982. Products of DNA cleavage by the 1,10-phenanthroline–copper complex. *J Biol Chem 257*:12121–12128.

Sigman DS, Chen CB. 1990. Chemical nucleases: New reagents in molecular biology. *Annu Rev Biochem 59*:207–236.

Sigman DS, Spassky A, Rimsky S, Buc H. 1985. Conformational analysis of lac promoters using the nuclease activity of 1,10-phenanthroline–copper ion. *Biopolymers 24*:183–197.

Singh UC, Kollman PA. 1984. An approach to computing electrostatic charges for molecules. *J Comput Chem 5*:129–145.

Singh UC, Weiner SJ, Kollman PA. 1985. Molecular dynamics simulations of d(C-G-C-G-A)*d(T-C-G-C-G) with and without "hydrated" counterions. *Proc Natl Acad Sci USA 82*:755–759.

Stockert JC. 1989. An intercalative and minor groove binding model for the DNA cleavage reagent, copper(I) (1,10-phenanthroline)$_2$. *J Theor Biol 137*:107–111.

Sussman JL, Holbrook SR, Warrant RW, Church GM, Kim SH. 1978. Crystal structure of yeast phenylalanine transfer RNA. *J Mol Biol 123*:607–630.

Tanner NK, Schaff S, Thill G, Petit-Koskas E, Crain-Denoyelle AM, Westhof E. 1994. A three-dimensional model of hepatitis delta virus ribozyme based on biochemical and mutational analyses. *Curr Biology 4*:488–498.

Thederahn TB, Kuwabara MD, Larsen TA, Sigman DS. 1989. Nuclease activity of 1,10-phenanthroline–copper: Kinetic mechanism. *J Am Chem Soc 111*:4941–4946.

Veal JM, Rill RL. 1989. Sequence specificity of DNA cleavage by bis(1,10-phenanthroline)copper(I): Effects of single base pair transitions on the cleavage of preferred pyrimidine-purine-pyrimidine triplets. *Biochemistry 28*:3243–3250.

Wang JF, Cech TR. 1992. Tertiary structure around the guanosine-binding site of the *Tetrahymena* ribozyme. *Science 256*:526–529.

Wang YH, Sczekan SR, Theil EC. 1990. Structure of the 5′ untranslated regulatory region of ferritin mRNA studied in solution. *Nucleic Acids Res 18*:4463–4468.

Weiner SJ, Kollman PA, Case DA, Singh UC, Ghio C, Alagona G, Profeta S, Weiner P. 1984. A new force field for molecular mechanical simulation of nucleic acids and proteins. *J Am Chem Soc 106*:765–784.

Weiner SJ, Kollman PA, Nguyen DT, Case DA. 1986. An all atom force field for simulations of proteins and nucleic acids. *J Comput Chem 7*:230–252.

Westhof E, Dumas P, Moras D. 1988. Restrained refinement of two crystalline forms of yeast aspartic acid and phenylalanine transfer RNA crystals. *Acta Crystallogr A 44*:112–123.

Westhof E, Romby P, Ehresmann C, Ehresmann B. 1990. Computer-aided structural biochemistry of ribonucleic acids. In: Beveridge DL, Lavery R, eds. *Theoretical biochemistry & molecular biophysics*. New York: Adenine Press. pp 399–409.

Determination of nucleotide distances in RNA by means of copper phenanthroline-generated hydroxyl radical cleavage pattern.

T Hermann and H Heumann

RNA 1995 1: 1009-1017